Anatomy of a slip event in an idealized fault gouge

David Sparks[(1)] and Einat Aharonov[(2)]

(1) Department of Geology and Geophysics, Texas A&M University, College Station, Texas, USA (e-mail: sparks@seaver.tamu.edu, phone +1-979-458-1051, fax: +1-979-845-6162). (2) Environmental Sciences and Energy Research Department, Weizmann Institute of Science, Rehovot, Israel (email:einata@wicc.weizmann.ac.il).

Abstract

Two-dimensional numerical simulations of shear in a layer of frictional grains were conducted to illuminate the micromechanics of deformation in granular materials (such as layers of fault gouge) during "stick-slip" motion. We found that, while the largest intergranular forces in the system are between sets of grains aligned with the direction of maximum compression ("force chain grains"), the triggering mechanism for a slip event may reside in the grains that lie between force chains. As stress on the system increases, the "weak" contacts that are not in force chains accumulate enough shear force to reach the frictional sliding limit, while the force chain ("strong") contacts never reach this limit. It is suggested that when enough of the non-chain grains can frictionally slide, this material fluidizes, which destabilizes the force chains.

Introduction

Natural faults with significant displacement are often filled with a layer of gouge, that thickens with increasing strain.. Since unstable sliding, or "stick-slip" motion, is characteristic of many natural gouge-filled faults, (cf. Mair and Marone, 1999[1]) it is important to have a fundamental understanding of the micromechanics of gouge deformation under these circumstances. Despite interest in this problem, it has eluded complete understanding due to the complex nature of granular materials.

In a densely-packed granular layer, stress will be transmitted across the system by a network of "force chains", or sublinear sets of grains which interact through long-lasting contacts that each carry up to several times the mean contact force. The majority of grains in the layer will lie between force chains and may weakly interact with the force chains and with each other. Force chains tend to preferentially align with the direction of maximum compressive stress in the system. Because of this, they can support large loads along their axis, but may be weak to other kinds of applied loads. This conditional instability has led to the description of such granular material as a "fragile" state of matter (Cates et al., 1998[2]) consisting of force chains and "spectator" grains.

In describing the strength of a granular material, much attention has been focused on force chains (e.g. Sammis and Steacy, 1994[3], Cates et al., 1998[2]). This is understandable since experimentally it is much easier to observe the large contact forces in a system than the small forces. In order for significant deformation to occur, involving permanent rearrangement of grains, force chains must be destroyed. In a continuously shearing granular material, force chains always exist, since they are what maintains the volume of the layer against applied confining forces. However, individual chains. are created and destroyed very rapidly, at a rate even larger than large-scale grain

rearrangement. In this paper, we will suggest that the loss of strength that triggers a slip event during stick-slip motion is initiated by changes in the orientation of the weaker contact forces between force chains and the surrounding grains.

A numerical model of stick-slip in granular layers

We describe simple two-dimensional numerical experiments that are similar in design to those of Thompson and Grest (1991)[4], and the laboratory experiments of Nasuno et al. (1998)[5] study. The numerical techniques used in these models are very similar to those used in a previous paper (Aharonov and Sparks, 1999[6]). We use the discrete element method (cf. Cundall, 1979[7]),which treats grains as inelastic disks with rotational and translational degrees of freedom.

In our formulation, distance is measured in units of average disk diameter, $\overline{R}$, time is scaled by the undissipated elastic wave travel time across this distance scale, velocity is scaled by the elastic wave speed, and force by the elastic repulsive force between grains. The simulations were performed in roughly square systems with about 550 (24x24) grains. The top and bottom boundaries of the layer were composed of grains glued together along their centerlines to form rigid rough walls. The system was periodic in the horizontal direction. Polydispersivity was introduced to discourage ordering effects: the grain sizes were normally distributed, and ranged over a factor of three in diameter. The systems were initiated as tall loosely packed boxes, which were compacted vertically by applying normal stress to the top walls.

In order to allow stick-slip motion of the system, the top wall is driven by a time-varying horizontal force on the top wall, which simulates driving by a spring attached to the upper wall. The other end of the spring is pulled to the right at a constant velocity V_{sp}. The horizontal velocity of the bottom wall is fixed at zero, and a vertical normal stress N is applied to both walls. Under certain conditions of spring velocity and applied normal force, the wall moves in a stick-slip manner.

We ran series of numerical experiments at a range of pulling velocities, spring constants, and normal stresses. Stick-slip motion in our experiments is characterized by a saw-tooth pattern in the shear resistance force, and short periods of rapid "slip" (up to an order of magnitude faster than V_{sp}) separated by variable-length "stick" periods, in which the wall velocity is less than $10^{-2}V_{sp}$. The slip distance can vary within an experiment from 1 to 10 grain diameters, but is typically 4-5.

Contact statistics

During a slip event, several characteristics of the system (porosity, coordination number, density of force chains) change rapidly and dramatically. However, during the stick period, none of these measures show a consistent pattern of evolution toward a critical value or rate of change that predicts that a slip event is imminent.

To determine the dynamics during a slip event, we examine the distribution of intergranular contact orientations and forces. In this we follow the analysis introduced by Rothenburg and Bathurst (1989)[8] and used by Radjai et al. (1998)[9]. Because of the nature of packing of heterogeneous grains, the direction and magnitude of force on contacts between grains is highly variable. A statistical approach is required to determine if a set of contacts has a preferred orientation. Rothenburg and Bathurst (1988)[8] defined the probability $P(\theta)$, of finding a contact with direction θ within the set of contacts by

$$P(\theta) = \frac{1}{2\pi}\left[1 + A\cos 2(\theta - \theta_0)\right] \quad (1)$$

where θ_0 is the angle of the preferred orientation, and A is a parameter determining the magnitude of the anisotropy of contact directions. A increases roughly proportional to the difference between the number of contacts that are parallel to and perpendicular to θ_0; i.e., $A = 0$ corresponds to a random distribution. At a given instant during the run, we sort the contacts by the total force, F, and calculate, among other things the amplitude and direction of preferred orientation of subsets of contacts, the average stress state on the contacts and the fraction of those contacts that are slipping frictionally.

Radjai et al. (1998)[9] demonstrated for a box of grains deformed in pure shear that there was a natural division of contacts at the mean contact force, $<F>$. The degree and direction of preferred orientation among the "weak" contacts ($F < <F>$), was different from that among the "strong" contacts ($F > <F>$), with the latter oriented in the direction of the maximum principle compression, and the former in the direction of minimum principle compression. We see similar distribution of forces during part of our stick-slip experiment, but over time there are significant changes in the weak network that will be discussed below. We use the terms "strong" and "weak" here only in reference to the magnitude of the contact force relative to the mean of the system; however, it will be shown that this measure correlates well with the frictional sliding stability of the contact. The strong contacts can be identified as those between grains in system-spanning force chains, while the weak contacts involve grains that are not in a force chain.

We will examine a section of a single numerical simulation, focusing on one slip event and the stick period following it. During this section, information about the grains and forces were output at small, evenly-spaced time intervals, which will be referred to by frame numbers to ease description. The slip event described below occurred between frames 14 and 25, and the system was then stuck until the next slip event at frame 105.. The dimensionless driving velocity of the spring in this experiment was $3\text{x}10^{-4}$, but the peak wall velocity during the slip even was about $6\text{x}10^{-3}$.

To highlight the differences between the weak and strong contacts, we calculate statistics for the set of all the contacts with a force below a prescribed value, F_c (which ranges from a small cutoff value to the maximum value of F in the system). Therefore, when $F_c / <F> = 1$, the plots show statistics for all the 'weak' contacts, with forces at or below the mean. At the maximum value of $F_c / <F>$ (between 4 and 5), the plots show the statistics for all the contacts in the system ('weak' and 'strong'). This cumulative approach is taken to avoid the problems due to the possibly small numbers of contacts within any given force interval (Radjai, 1996)[10].

Each curve in Figure 1 plots an average over a subset of contacts vs. the upper limit of the force defining the subset (F_c) at a particular time (frame). The three frames shown here (13, 15 and 17) occur during the beginning of the first large slip event. The wall velocity in this time period changes from $4.4\text{x}10^{-5}$ to $1.1\text{x}10^{-3}$ to $3.4\text{x}10^{-3}$, respectively. The total dimensionless displacement of the top wall between frames 13 and 15 is 0.153 R, less than 2% of the total displacement during the slip event.

In frame 13, the magnitude of anisotropy is large for very weak forces, approaches zero near $F_c/<F>=1$, then increases at larger forces (Figure 1a). This is because there is preferred orientation to both the strong and moderately weak ($F_c / <F> < \sim 0.75$) contacts but the direction of those contacts is opposite to each other. The direction of the strong contact forces is about 45 from horizontal, in the expected direction of maximum principle compression for a system undergoing shear. However, the orientation of the weak forces is at approximately right angles to the strong ones. This distribution of contact orientations is the same as that seen in simulations of similar to that of a system deformed in continuous pure shear (Radjai, 1998)[9].

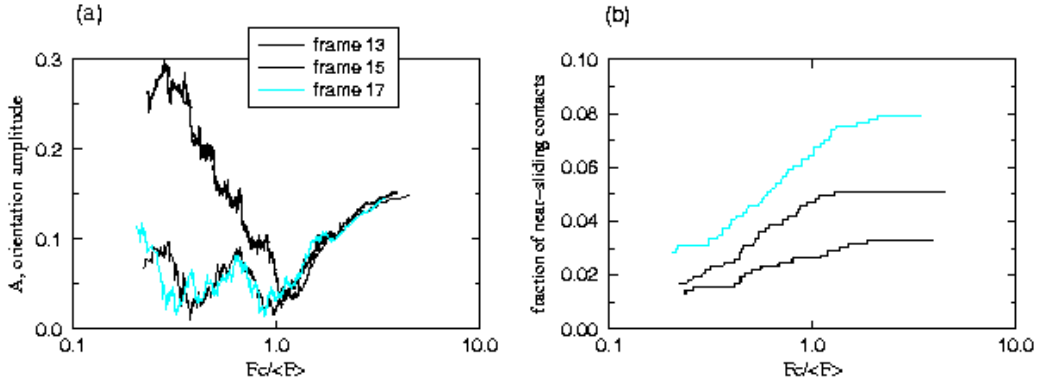

Fig. 1. (a) The extent of preferred orientation, and (b) the fraction of the total contacts that are in a frictional sliding state in subsets of intergranular contacts with force less F_c. The three lines on each plot represent three different frames, or time slices near the beginning of a "slip" event.

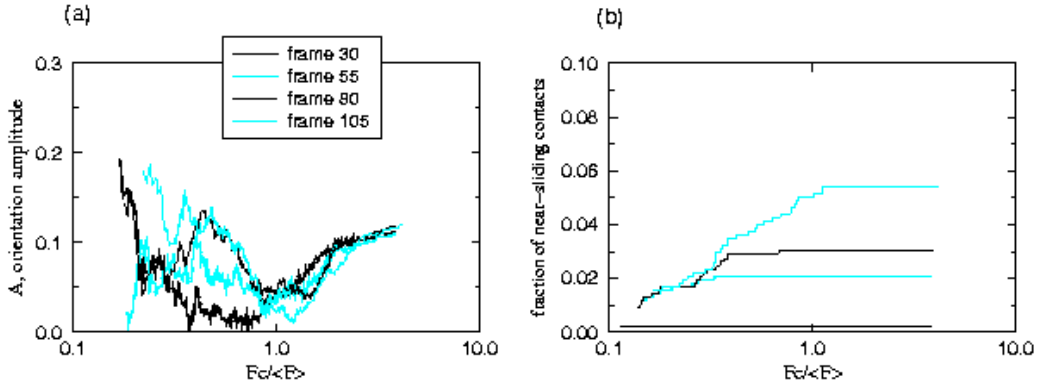

Fig. 2. The same statistics shown in Figure 1, plotted for four frames during the "stick" period.

However, this arrangement changes at the onset of slip. In frame 15 the degree of preferred orientation of the weak contacts has dropped considerably, indicating that the weak contacts have become more nearly randomly oriented. There is also a decrease in the deviatoric stress supported by the set of weak contacts; i.e. the average stress field imparted by the set of weak contacts becomes more nearly hydrostatic. This reduction in the anisotropy and average deviatoric stress in the network of weak contacts indicates that the non-force chain grains are switching from a solid-like state to a fluidized state.

Figure 1b shows the number of near-sliding contacts within a particular subset of contacts, normalized by the total number of contacts in the system. The total number of near-sliding contacts increases as slip initiates. However, almost all of the sliding occurs on weak contacts. None of the strongest contacts are near their sliding criterion (which is not surprising since they have the largest normal forces). This last observation is true for all the frames examined in this experiment, and indicates that frictional sliding is a mechanism that only occurs on weak contacts, and is not important for breaking contacts in force chains. In fact, the orientation and stresses in the strong, force-chain contacts remain relatively unchanged throughout the slip.

By the end of the slip event, the amount degree of preferred orientation in the set of weak contacts is nearly zero. Also the fraction of near-sliding contacts has dropped to near zero.

Figure 2 shows the much slower evolution of the contact statistics during the stick period leading up the next slip event, at about frame 105. The wall velocities during these frames are all below 10^{-4}. At the end of the slip period (frame 30), the weak contacts are nearly randomly distributed, with almost no sliding contacts. As time progresses during the stick period, shear stress on the system builds back up. This results in a gradual realignment of weak contacts to perpendicular to maximum compressive stress. Shear stress on the contacts increases, putting an increasingly larger number of contacts in a near-sliding condition. The weakest contacts are the first to reach the sliding condition, with the rollover in the curve migrating to larger F_c (Figure 2b). This is in contrast to system that is in a quasi-steady state, either a static packing (Radjai et al., 1996)[10] or a system deformed at constant velocity (Aharonov and Sparks, in prep.); in these situations the fraction of sliding contacts is independent of F_c.

To summarize the difference between the stick state and the slip state: at the beginning of the slip event, the contacts with weak forces (non-force chain contacts) are preferentially aligned at right angles to maximum compression (the force chain direction), and they support deviatoric stress. As slip occurs, these contacts become more randomly oriented, and the stresses in these contacts become more hydrostatic, as they would in a fluid phase.

Discussion

The analysis of the contact forces during and after a slip event suggests that, while force chains are definitely broken and reformed during a slip event, the critical process that allows this to occur (and therefore slip to begin) is the fluidization of the grains that are not in stress chains. During a stick period of stress buildup, these grains preferentially exert forces on the sides of the force chains, stabilizing them under an increasing load. Meanwhile an increasing number of contacts between these grains reach the frictional sliding limit, until at the onset of slip, these grains fluidize. Further numerical work using larger systems and examining many events is under way, and may clarify this process.

The fate and role of force chains is still an outstanding question. We know that no single force chain with a fixed set of grains can exist throughout a slip event which displaces the upper wall by several grain diameters. In fact, most force chains don't survive even very small displacements. Yet the distribution and preferred orientation of strong contacts is maintained. Therefore force chains are obviously destroyed and created continuously during a slip event. We have seen that the strong contacts don't slide frictionally. While dilation does occur, this puts additional compressive forces on the chains, precluding an opening mechanism for their destruction. We suggest that force chains do not "break" so much as they are superceded by new chains of grains that more advantageously arranged to support the stress on the system. These new chains can form during slip because of the mobilization of the grains between force chains. As the original chains are rotated by deformation, new chains consisting of new sets of grains form and relieve the stress on the old chains. This could explain the observation that the small change in the angle of preferred orientation during slip is positive, i.e. toward horizontal, instead of toward vertical as would be expected from chain rotation.

An interesting question that arises from the fluidization of the non-chain grains is the role of fluids in natural gouge systems. Enhanced fluid pressure in the pores between these grains could affect the rate at which fluidization occurs, or conversely the gradual reorientation of contacts among these grains during stress loading could lead to permeability or conductivity variations and anisotropies that could signal the current stability state of a fault.

Acknowledgements

This research was funded by NSF grant EAR98-04855.

References

[1] Mair, K., and C. Marone, 1999,*Friction of simulated fault gouge for a wide range of velocities and normal stresses*, J. Geophys. Res., **104**, 28899-28914.
[2] Cates, M.E., J. Wittmer, J. Bouchaud, and P. Claudin, 1998, *Jamming, force chains, and fragile matter*, Phys. Rev. Lett., **81**, 1841-1844.
[3] Sammis, C. G., and S. J. Steacy, 1994,*The micromechanics of friction in a granular layer,* Pure and Appl. Geoph., **142**, 777-794.
[4] Thompson, P. A., and G. S. Grest, 1991,*Granular flow: friction and the dilatancy transition*, Phys. Rev. Lett., **67**.
[5] Nasuno, S., A. Kudrolli, A. Bak, and J. P. Gollub, 1998, *Time-resolved studies of stick-slip friction in sheared granular layers*, Phys. Rev. E., ***58***.
[6] Aharonov, E., and D. W. Sparks, 1999, *Rigidity phase transition in granular packings*, Phys. Rev. E, **60**, 6890-6896.
[7] Cundall, P. A., and O. D. Strack, 1979, *A discrete numerical model for granular assemblies*, Geotechnique, **29**, 47-65,.
[8] Rothenburg. L., and R. J. Bathurst, 1989, Geotechnique, **4**, 601.
[9] Radjai, F., D. Wolf, M. Jean, and J. J. Moreau, 1998, *Bimodal character of stress transmission in granular packings,* Phys. Rev. Lett., **80**.
[10] Radjai, F., M. Jean, J. J. Moreau, and S. Roux, 1996, *Force distributions in dense two-dimensional granular systems*, Phys. Rev. Lett., **77**, 274-277.